CONTACTLESS MEASUREMENT OF HEART RATE VARIABILITY FROM PUPILLARY FLUCTUATIONS

Avinash Parnandi and Ricardo Gutierrez-Osuna

Department of Computer Science and Engineering, Texas A&M University
{parnandi,rgutier}@tamu.edu

ABSTRACT

The ability to measure a person's physiological parameters in a contactless fashion without attaching electrodes to the skin has tremendous potential in making healthcare delivery more efficient. In this paper, we present a proof-of-concept method for measuring one such vital parameter, heart rate variability (HRV), in a contactless fashion from the spontaneous pupillary fluctuations. Pupillary measurements are done using a remote eye tracker for imaging and an integro-differential algorithm for the segmentation of the pupil-iris boundary. We estimate HRV from energy distribution in the low frequency (LF) (0.04 to 0.15 Hz) and high frequency (HF) (0.15 to 0.4 Hz) bands of the power spectrum of the pupillary fluctuations. In our study, we noted statistically significant correlation between the estimated HRV and the ground truth measures under a range of breathing conditions and under different illumination levels. The high degree of agreement evident in our results suggests that pupillary fluctuations obtained in a contactless fashion can be a reliable indicator of HRV.

Index Terms— Contactless sensors, physiological sensing, heart rate variability, pupillometry

1. INTRODUCTION

Physiological parameters provide important information on the health, emotional, and cognitive state of a person. Parameters such R-R beat interval, heart rate variability (HRV) or electro-dermal activity (EDA) are all indicators of modulation in the autonomic nervous system (ANS) [1]. Physiological signals are also widely used for health and fitness monitoring, stress assessment, psychophysiological studies, and a multitude of other applications. Among the different physiological variables, HRV is of special significance because it provides important information about the cardiovascular regulation by the ANS, and for the diagnosis of cardiac and other chronic and acute diseases [2].

HRV measurement with existing technologies is obtrusive, as it requires skin contact via electrodes, chest straps, finger clips etc. It can further be uncomfortable to the subject, and some sensor modalities (e.g., pulse oximetry) can even restrict activities of daily living. Contactless physiological sensing, that is, remotely measuring vital parameters without affixed electrodes to patients' skin, can provide a viable solution to these problems. Besides being unobtrusive, contactless sensors can have an additional potential benefit of reducing contact artifacts caused by the electrodes.

In this paper, we target the problem of contactless measurement of HRV. Our approach relies on measuring fluctuations in pupil diameter , which are typically modulated by cardiopulmonary rhythms [3]. For this purpose, we use a remote/desktop eye-tracker to image the eyes from which the pupillary information is extracted. We then use the Viola-Jones algorithm [4] for eye detection in the images and the Daugman's integro-differential operator [5] to extract pupil and iris centers and radii. Finally, we analyze the power spectrum density (PSD) of pupil dilation in the LF and HF bands to estimate HRV. Our results show statistically significant correlations between the pupil-based contactless measurement of HRV and ground truth measurements from a commercial heart-rate monitor. We also illustrate the robustness of the method under different ambient illumination levels, to which pupil dilation is very sensitive.

Relation to prior work: Our work is motivated by the limitations of the existing methods for contactless physiological sensing which mainly use radar-based techniques ([6-9]). These methods can provide reliable readings but are limited in that even small involuntary body movements can significantly reduce the signal-to-noise ratio (SNR). In contrast with radar-based approaches, our proposed method operates in the optical domain by measuring pupillary fluctuations. Prior research correlating pupil size and physiological variables has had one major limitation in that it makes assumptions about the ambient illumination levels [10-12]. As opposed to these, our approach measures pupillary fluctuation in a contactless fashion. Because we work in the frequency domain by focusing on pupillary fluctuations, as opposed to absolute pupil diameter, our system is robust to illumination conditions as well as scale/resolution differences.

2. BACKGROUND AND PRIOR WORK

Heart rate variability (HRV) is the physiological phenomenon of variation in the beat-to-beat (R-R) intervals. It is one of the most widely used quantitative markers of cardiovascular regulation by the autonomic nervous system (ANS). Analysis of HRV can provide important information in the diagnosis of cardiac and other chronic and acute diseases. HRV measures are also widely used in psychophysiology as an indicator of autonomic balance: activation of the sympathetic nervous system (SNS) branch leads to reduction in HRV (fight/flight response), while activation of the parasympathetic nervous system (PNS) component is associated with increases in HRV [1, 2].

Pupil is an aperture in the iris that regulates the amount of light entering the eye. Pupil size can be affected by two factors: optical responses and fluctuations caused by ANS. The pupillary optical response comprises of light reflex, which controls the diameter of the pupil in response to illumination levels, and the accommodation response, which changes the curvature of the lens

to control the depth of field. In turn, activation and inhibition of the two ANS branches lead to small-scale spontaneous pupillary fluctuations known as hippus [13]; these fluctuations are the target of our study.

2.1 Literature review

Various approaches have been developed for contactless physiological sensing, including radar-based sensors, thermal imaging and, more recently, web cameras. In early work, Grenecker [8] presented an active sensing technique for noncontact measurement of breathing rate. The author used Doppler-modulated radar to sense the shock wave reflecting off the chest wall expansion and contraction during breathing. More recently, Droitcour developed a low-power sensor for measuring cardio-respiratory rates [6] using microwave Doppler radar. These radar-based methods rely on detecting small skin/organ displacements resulting from cardiopulmonary pulses, so they are rather sensitive to motion artifacts. As an example, seemingly small body motion can produce much larger Doppler-modulated radar cross-sections than those caused by the physiological motion of interest. Pavlidis and colleagues have used high-end thermal imaging cameras to measure a variety of physiological variables, including vessel blood flow, cardiac pulse, breathing rate [14]; their methods have been used for large-scale screening in homeland security applications [15, 16]. Recently, Poh et al. [17] used consumer web cameras for non-contact measurement of HR, breathing rate, and HRV. The authors showed how fluctuations in the RGB color channels of facial images correlate with various physiological variables.

Pupillometry has been widely used in medical and psychophysiology studies. In early work, Ohtsuka et al. [10] found correlation between respiration and fluctuations in pupil diameter. Nakayama et al. [18] performed frequency analysis on the pupillary response and eye movement to study the effect of mental workload. Their study showed a significant increase in power spectral density (0.1–0.5 Hz) with task difficulty. The transient pupil light reflex (PLR) has been used for the assessment of autonomic function in athletes, autistic and healthy children [12, 19, 20]. Fan et al. [12] compared the PLR profiles between autistic children and children with typical development. They found autistic group to have significantly longer PLR latency. Filipe et al. [19] evaluated autonomic functions in athletes using PLR parameters which included reflex amplitude, pupil redilation time, constriction and redilation velocity) .

3. METHODS

An overview of our approach for contactless measurement of heart-rate variability is illustrated in Figure 1. In a first step, we localize the eye in the image using the Viola-Jones multi-scale object detector [4]. The method uses Haar-like features to encode details, which are then used with a cascade of classifiers to locate the presence of the target object (eye) in the given image. Once the eye has been located, we preprocess the image to remove the corneal reflections. Next we detect the pupil-iris boundary using an integro-differential operator, which allows us to compute the pupil diameter. The image processing is illustrated in Figure 1 (bottom). In a final step, we perform spectral analysis of the fluctuations in pupil diameter to extract an index of HRV.
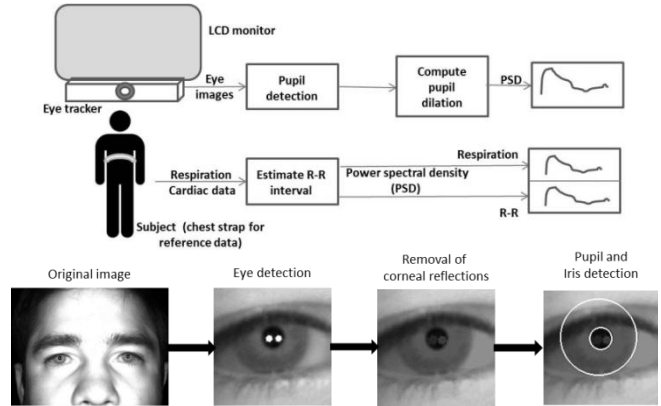

Figure 1: Overview of the method

The critical step in the process is accurately detecting the pupil and iris center and their respective boundaries. These are challenging problems because of issues such as occlusion by the eye lids and eye lashes, corneal reflections, color of the eye, imaging angle, etc. [21]. A few approaches have been developed for this purpose, which mainly use variants of Hough transform and active contours [22, 23]. Hough transform based methods require threshold value selection for edge detection which can lead to failures with off-axis and noisy images. Similarly, active contour models can lead to false contours because of eyelids and eyelashes [23].

To address the limitations of conventional methods for iris detection, we used a method originally proposed by Daugman [5] that is robust to occlusions caused by the upper and lower eyelids. The algorithm assumes the pupil and iris have circular geometry, and uses an integro-differential operator to locate the boundaries between them:

$$\{r, x_0, y_0\} = \operatorname*{argmax}_{r, x_0, y_0} \left| G_\sigma(r) * \frac{\partial}{\partial r} \oint_{r, x_0, y_0} \frac{I(x, y)}{2\pi r} \, ds \right| \qquad (1)$$

where $I(x, y)$ is the image and $G_\sigma(r)$ is a smoothing gaussian kernel. The three parameters: x_0, y_0 (center) and r (radius) define the path of the contour for integration.

Equation (1) essentially acts as a circular edge detector: it iteratively searches for a maximum contour integral derivative with increasing radius of the circular contour in image space. Namely, a circular projection is obtained at every location of the eye image, and the differential value of the projection is computed. The differential values are then convolved with the gaussian kernel for smoothing. The circular contour with maximum change in pixel intensity results in the largest convolved differential value; this is taken as the estimated boundary. To locate the iris and pupil, the spread parameter σ in the smoothing gaussian kernel takes two distinct values. In a first step, the operator uses a coarse value to find the pronounced boundary between the iris and the sclera. Detecting the iris-sclera boundary considerably reduces the ROI for locating the pupil-iris boundary, which requires a much finer spread parameter.

For efficient implementation, we interchange the order of differentiation and convolution in eq. (1) and concatenate them. To discretize eq. (1), we then use the finite difference approximation of the derivative operator:

$$\frac{\partial G_\sigma(r)}{\partial r} \cong \frac{1}{\Delta r} G_\sigma(n\Delta r) - \frac{1}{\Delta r} G_\sigma((n-1)\Delta r) \qquad (2)$$

then we replace the convolution and integral with summations resulting in equation (3) (shown at the bottom of the page). In eq.(3), Δr is a small increment in the radius, $\Delta\theta$ is the angular sampling interval along the circular arcs, K is the convolution shift parameter, and $(k\Delta r\ \cos(m\Delta\theta) + x_0)$, $k\Delta r\ \sin(m\Delta\theta) + y_0)$ represents a point on the circular contour.

Although this algorithm is a robust technique for detection of the pupil, it can be susceptible to corneal specular reflection . To address this issue we add a preprocessing step to first detect the reflections as holes and then fill them using a flood-fill operation. This operation brings the intensity of the light area that are surrounded by darker areas upto the same intensity level as the surrounding pixels. This corresponds to removing regional extremums that are not connected to the image border.

4. EXPERIMENTAL

To validate our methods, we used a low-cost eye tracking system with IR illumination (easyGaze; Design Interactive, Inc.). The eye-tracker consists of an IR sensitive camera (resolution 1280×960, 16 FPS) and arrays of IR LEDs (power: 1 mW/cm^2, wavelength: 850 nm) which are offset from the optical axis. The off-axis setup causes the IR light reflection to be projected away from the camera; this makes the pupil darker than the iris and the sclera lighter than the iris, thus enabling accurate segmentation of the pupil and iris boundaries. We also used a Zephyr Bioharness BT chest strap heart rate sensor (sampling rate: 18 Hz) to obtain ground truth measures of HRV and respiration.

Before doing spectral analysis, we preprocess the pupillary and cardiac signals to address irregular and burst sampling. As occurrences of R-wave are not equidistantly timed events, this results in irregularly sampled R-R interval time series, which cannot be used directly for spectral analysis. We performed bicubic interpolation on the signal to resample it into a uniformly timed series. Similarly we interpolated the pupillary time series to account for missing frames and non-uniform sampling. After resampling, we compute pupil dilation by subtracting the current pupil diameter from a baseline value, measured as the average pupil diameter computed over the past 1.5 seconds using a sliding window. We chose this duration because it is a good approximation of the response time of the pupil to a stimulus [1].

4.1 Protocol

The study was conducted on 5 subjects, all male, between the ages of 22-28 years and was approved by the Texas A&M Institutional Review Board. The experiments were performed indoors with participants seated on an adjustable chair in front of the remote eye tracker at a distance of approximately 2 feet. Figure 1 illustrates our experimental setup.

The experiments were divided into two phases. In the first phase, we conducted the experiments under paced breathing at 6, 9, 12 breaths per minute (bpm) as well as under spontaneous breathing. For paced breathing, we used an audio pacing signal which guided the subjects to inspire/expire at appropriate times to maintain the desired breathing pace. For spontaneous breathing, no pacing signal was used, e.g., subjects were allowed to breathe at their own pace. Pupillary, cardiac, and breathing data was collected for 5 minutes under each breathing condition for each subject. In the second phase, we evaluated our method under two illumination
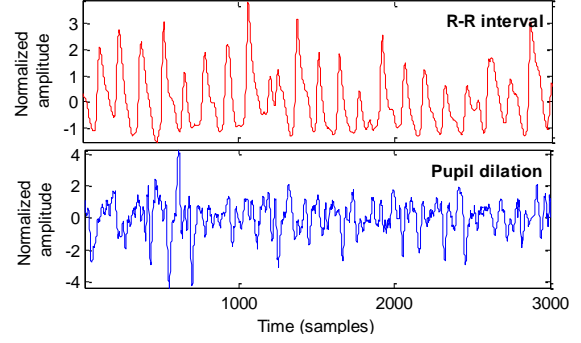

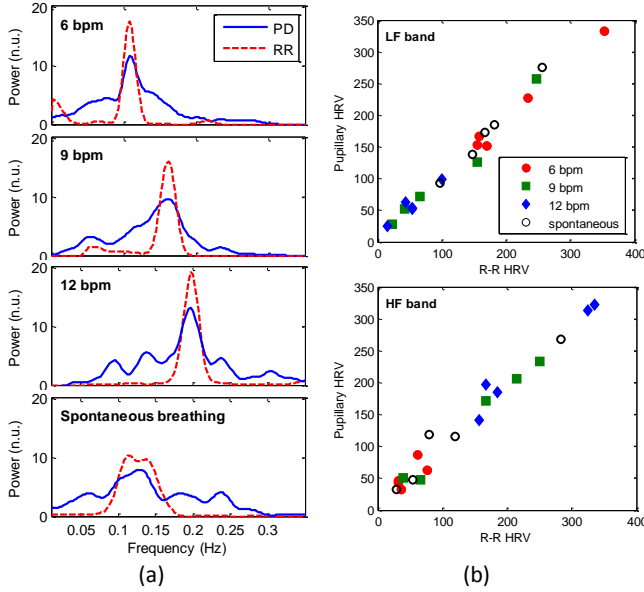**Figure 2:** R-R interval and pupil dilation time series

levels (high and low) set by modifying the brightness and color of two 22" LCD monitors placed at a distance of 3 feet from the subject. For the high illumination condition both screens displayed white color at maximum brightness, whereas for the low illumination condition they displayed a black color with minimum brightness. During phase two, participants were asked to follow a 9 bpm breathing pacing signal.

5. DATA ANALYSIS AND RESULTS

As pupillary fluctuations and R-R interval are both influenced by ANS activity, we hypothesized a strong correlation between the two signals. Analysis in the temporal domain, however, does not reveal such correlation between the two signals –see Figure 2. As a result, using time-domain measures of HRV such as RMSSD (root mean square of the successive differences) [2] to analyze pupillary dilation (PD) is likely to be ineffective. Instead, our method focuses on HRV measures based on frequency-domain analysis. Figure 3 shows the power spectral density (PSD) of the two signals under different breathing paces (6, 9, 12 bpm) and under spontaneous breathing in normalized units (n.u.). Under paced breathing (see Figure 3(a)), each signal (RR interval: red; PD: blue) shows a prominent peak at the specified breathing rates. The pupillary PSD, however, shows a broader spectral peak; this result is to be expected given the higher noise levels shown in the time-domain signal of Figure 2. Under spontaneous breathing – Figure 3(a) bottom, both signals also have a much wider spectral spread compared to the paced breathing condition. This result is also reasonable since under spontaneous breathing the breathing rate for each subject changes over time. Overall, though, these plots show that under both paced and spontaneous breathing conditions, there is significant overlap between the RR and PD spectra, which indicates that the PD spectra can be used to compute HRV.

To verify our visual inspection of the results in Figure 3, we extracted two spectral features of HRV from both signals: energy in the HF band (0.15 to 0.4 Hz) and in the LF (0.04 to 0.15 Hz) bands. Results are shown in Figure 3(b). The x-axis of the scatter plots represents the HRV features from the contact sensor (RR), while the y-axis shows the HRV obtained from the contactless method (PD). A strong correlation between the two measures is evident in both bands. The correlation coefficient between the estimated HRV and ground truth was found to be $r = 0.98$ for the LF and $r = 0.97$ for the HF band ($p < 0.001$ in

$$\{n\Delta r, x_0, y_0\} = \underset{n\Delta r, x_0, y_0}{\operatorname{argmax}} \left| \frac{1}{\Delta r} \sum_k \left\{ \left(G_\sigma\big((n-k)\Delta r\big) - G_\sigma\big((n-k-1)\Delta r\big) \right) \sum_m I[k\Delta r\ \cos(m\Delta\theta) + x_0),\ k\Delta r\ \sin(m\Delta\theta) + y_0)] \right\} \right| \quad (3)$$

Figure 3: (a) Power spectra of R-R interval, and pupillary fluctuations for different breathing rates (1 subject). (b) HRV from pupil and R-R for all subjects.

both cases).

5.1 Robustness to illumination intensity

Pupillary size is highly sensitive to ambient light intensity. As a result, psychophysiological variables derived from the absolute pupil diameter (e.g., mental workload) must be measured under controlled lighting conditions. However, because our approach relies on fluctuations in pupil diameter we hypothesized that it would be robust to lighting conditions.

Figure 4(a) shows the time-domain signal for pupillary size (one subject) under the low and high illumination conditions described in section 4.1. With high illumination, the pupil diameter is reduced to limit the amount of light entering the eye; in contrast, with low illumination, the pupil diameter becomes larger to allow more light. Clearly, any measure relying on absolute pupillary size will have to account for the ambient light intensity. Figure 4(a) shows that fluctuations in PD are also affected by the ambient light: the amplitude of the fluctuations is smaller under high illumination; this is because under high illumination the pupil is already constricted to a small radius thus restricting further large fluctuations leading to a lower spectrum. However, the frequency of the fluctuations remains constant in both cases. Figure 4(b) shows the power spectra of the RR interval and PD at high and low illumination levels (same subject as in Figure 4(a)). At both illumination levels, the power spectra shows a peak at 0.15 Hz (breathing rate: 9 bpm) though, as observed in the time-domain signals of Figure 4(a), the peak in the PD power spectra has a lower amplitude for the high illumination condition than for the low illumination condition. Overall, though, these results indicate that spectral analysis of PD fluctuations is robust to changes in illumination levels. Figure 4(c) shows the peak frequency for the RR and PD spectra under the two illumination levels for the five subjects. Regardless of illumination conditions (or individual differences across subjects) the spectra peaks at around 0.15 Hz which corresponds to the specified breathing rate of 9 bpm.
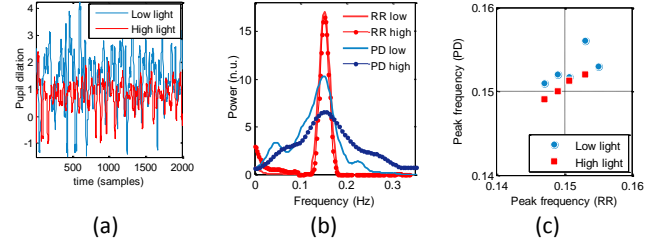
Figure 4: (a) PD in low and high light (1 subject) (a) Power spectra of RR and PD in L and H light (1 subject). (c) Peak frequency of RR and PD spectra in L and H light (5 subjects)

6. DISCUSSION AND CONCLUSION

We presented a proof of concept for measuring HRV from pupillary fluctuations in a contactless fashion. This method uses IR images of the eye from which the pupillary fluctuations are obtained. HRV is then computed from the power spectrum of the pupillary data. Our study demonstrated statistically significant correlation between the HRV measurements made from the pupillary spectrum and the ground truth values under a range of breathing conditions.

Along with breathing conditions, we also tested our method under different illumination levels. As explained in [1], the pupillary light reflex (PLR) constitute a major component in the overall pupillary response and is known to be larger in magnitude than spontaneous pupillary fluctuations caused by ANS. Because in this study we were utilizing the pupillary fluctuations as opposed to absolute pupil diameter we hypothesized that our method would be robust under different illumination conditions. With our experiments, we validated this hypothesis and obtained accurate results. This shows that useful physiological information can be extracted from the pupillary fluctuations spectrum even under different illumination levels.

The next logical step for us would be to evaluate the method under dynamic changes in illumination. In this case, the light reflex can be accounted for by integrating the PLR model [24] with our method. Such a model would express the pupil diameter as a function of the ambient lighting which can be subtracted to obtain the ANS component in pupillary fluctuations. In this work, we used a remote eye tracker for IR imaging but the eye-tracking capability on the device was not used or needed. Hence off-the-shelf IR webcams such as [25] or the IBM pupil-cam [26] can also be used instead which would theoretically provide similar performance.

Although we achieved high level of accuracy, the results should be considered in the light of the following issues. The current pupil detection algorithm has proven to be robust against minor head movements. However, other sources of inconsistencies such as rotation of the camera, and large movements might cause it to fail. Also, because it performs exhaustive search, even with a coarse-to-fine strategy the algorithm can be inefficient. The Adaboost-cascade iris detector suggested by He at al. [21] might provide an efficient alternative. Finally, our study was conducted with relatively small sample size and a longitudinal study would provide more insight and validate our method. From our results, it is however evident that HRV can be accurately computed from pupillary fluctuations in a contactless fashion and be potentially used for numerous real world applications.

4

7. REFERENCES

[1] J. T. Cacioppo, L. G. Tassinary, and G. Berntson, *Handbook of psychophysiology*: Cambridge University Press, 2007.

[2] T. Force, "Heart rate variability: standards of measurement, physiological interpretation and clinical use. Task Force of the European Society of Cardiology and the North American Society of Pacing and Electrophysiology," *Circulation,* vol. 93, pp. 1043-65, 1996.

[3] G. Calcagnini, S. Lino, F. Censi, and S. Cerutti, "Cardiovascular autonomic rhythms in spontaneous pupil fluctuations," in *Computers in Cardiology 1997*, 1997, pp. 133-136.

[4] P. Viola and M. Jones, "Rapid object detection using a boosted cascade of simple features," in *Proceedings of the IEEE Computer Society Conference on Computer Vision and Pattern Recognition. CVPR 2001. ,* 2001, pp. I-511-I-518 vol. 1.

[5] J. G. Daugman, "High confidence visual recognition of persons by a test of statistical independence," *IEEE Transactions on Pattern Analysis and Machine Intelligence,* vol. 15, pp. 1148-1161, 1993.

[6] A. D. Droitcour, "Non-contact measurement of heart and respiration rates with a single-chip microwave Doppler radar," Citeseer, 2006.

[7] M. Garbey, A. Merla, and I. Pavlidis, "Estimation of blood flow speed and vessel location from thermal video," in *Proceedings of the IEEE Computer Society Conference on Computer Vision and Pattern Recognition. CVPR 2004. ,* 2004, pp. I-356-I-363 Vol. 1.

[8] E. Greneker, "Radar sensing of heartbeat and respiration at a distance with applications of the technology," in *In Radar 97 (Conf. Publ. No. 449)*, 1997, pp. 150-154.

[9] D. Holdsworth, C. Norley, R. Frayne, D. Steinman, and B. Rutt, "Characterization of common carotid artery blood-flow waveforms in normal human subjects," *Physiological measurement 20.3 (1999),* vol. 20, p. 219, 1999.

[10] K. Ohtsuka, K. Asakura, H. Kawasaki, and M. Sawa, "Respiratory fluctuations of the human pupil," *Experimental Brain Research,* vol. 71, pp. 215-217, 1988.

[11] J. Klingner, R. Kumar, and P. Hanrahan, "Measuring the task-evoked pupillary response with a remote eye tracker," in *Proceedings of ETRA*, 2008, pp. 69-72.

[12] X. Fan, J. H. Miles, N. Takahashi, and G. Yao, "Abnormal transient pupillary light reflex in individuals with autism spectrum disorders," *Journal of autism and developmental disorders,* vol. 39, pp. 1499-1508, 2009.

[13] I. Loewenfeld and O. Lowenstein, "The light reflex," *The Pupil: Anatomy, Physiology and Clinical Applications,* pp. 189-193, 1993.

[14] M. Garbey, N. Sun, A. Merla, and I. Pavlidis, "Contact-free measurement of cardiac pulse based on the analysis of thermal imagery," *IEEE Transactions on Biomedical Engineering,* vol. 54, pp. 1418-1426, 2007.

[15] I. Pavlidis, N. L. Eberhardt, and J. A. Levine, "Seeing through the face of deception," *Nature,* vol. 415, pp. 35-35, 2002.

[16] P. Buddharaju, J. Dowdall, P. Tsiamyrtzis, D. Shastri, I. Pavlidis, and M. Frank, "Automatic thermal monitoring system (ATHEMOS) for deception detection," in *IEEE Computer Society Conference on Computer Vision and Pattern Recognition CVPR 2005.*, 2005, p. 1179 vol. 2.

[17] M. Z. Poh, D. J. McDuff, and R. W. Picard, "Advancements in noncontact, multiparameter physiological measurements using a webcam," *IEEE Transactions on Biomedical Engineering,* vol. 58, pp. 7-11, 2011.

[18] M. Nakayama and Y. Shimizu, "Frequency analysis of task evoked pupillary response and eye-movement," in *Proceedings of the symposium on Eye tracking research & applications. 2004*, 2004, pp. 71-76.

[19] J. A. Capão Filipe, F. Falcao-Reis, J. Castro-Correia, and H. Barros, "Assessment of autonomic function in high level athletes by pupillometry," *Autonomic Neuroscience,* vol. 104, pp. 66-72, 2003.

[20] K. C. Donaghue, M. Pena, A. Fung, M. Bonney, N. Howard, M. Silink*, et al.*, "The prospective assessment of autonomic nerve function by pupillometry in adolescents with type 1 diabetes mellitus," *Diabetic medicine,* vol. 12, pp. 868-873, 1995.

[21] Z. He, T. Tan, Z. Sun, and X. Qiu, "Toward accurate and fast iris segmentation for iris biometrics," *IEEE Transactions on Pattern Analysis and Machine Intelligence,* vol. 31, pp. 1670-1684, 2009.

[22] R. P. Wildes, J. C. Asmuth, G. L. Green, S. C. Hsu, R. J. Kolczynski, J. Matey*, et al.*, "A system for automated iris recognition," in *Proceedings of the Second IEEE Workshop on Applications of Computer Vision, 1994*, 1994, pp. 121-128.

[23] N. Ritter, R. Owens, J. Cooper, and P. P. Van Saarloos, "Location of the pupil-iris border in slit-lamp images of the cornea," in *Proceedings. International Conference on Image Analysis and Processing, 1999. ,* 1999, pp. 740-745.

[24] V. F. Pamplona, M. M. Oliveira, and G. V. G. Baranoski, "Photorealistic models for pupil light reflex and iridal pattern deformation," *ACM Transactions on Graphics (TOG),* vol. 28, p. 106, 2009.

[25] (2012). *Agama* Available: http://www.agamazone.com/products_v1325r.html

[26] C. H. Morimoto, D. Koons, A. Amir, and M. Flickner, "Pupil detection and tracking using multiple light sources," *Image and vision computing,* vol. 18, pp. 331-335, 2000.